

A Mutant Influenza Virus That Uses an N1 Neuraminidase as the Receptor-Binding Protein

Kathryn A. Hooper and Jesse D. Bloom
J. Virol. 2013, 87(23):12531. DOI: 10.1128/JVI.01889-13.
Published Ahead of Print 11 September 2013.

Updated information and services can be found at:
<http://jvi.asm.org/content/87/23/12531>

SUPPLEMENTAL MATERIAL

These include:

[Supplemental material](#)

REFERENCES

This article cites 29 articles, 19 of which can be accessed free
at: <http://jvi.asm.org/content/87/23/12531#ref-list-1>

CONTENT ALERTS

Receive: RSS Feeds, eTOCs, free email alerts (when new
articles cite this article), [more»](#)

Information about commercial reprint orders: <http://journals.asm.org/site/misc/reprints.xhtml>
To subscribe to to another ASM Journal go to: <http://journals.asm.org/site/subscriptions/>

A Mutant Influenza Virus That Uses an N1 Neuraminidase as the Receptor-Binding Protein

Kathryn A. Hooper,^{a,b} Jesse D. Bloom^{b,c}

Molecular and Cellular Biology Program, University of Washington, Seattle, Washington, USA^a; Division of Basic Sciences^b and Computational Biology Program,^c Fred Hutchinson Cancer Research Center, Seattle, Washington, USA

In the vast majority of influenza A viruses characterized to date, hemagglutinin (HA) is the receptor-binding and fusion protein, whereas neuraminidase (NA) is a receptor-cleaving protein that facilitates viral release but is expendable for entry. However, the NAs of some recent human H3N2 isolates have acquired receptor-binding activity via the mutation D151G, although these isolates also appear to retain the ability to bind receptors via HA. We report here the laboratory generation of a mutation (G147R) that enables an N1 NA to completely co-opt the receptor-binding function normally performed by HA. Viruses with this mutant NA grow to high titers even in the presence of extensive mutations to conserved residues in HA's receptor-binding pocket. When the receptor-binding NA is paired with this binding-deficient HA, viral infectivity and red blood cell agglutination are blocked by NA inhibitors. Furthermore, virus-like particles expressing only the receptor-binding NA agglutinate red blood cells in an NA-dependent manner. Although the G147R NA receptor-binding mutant virus that we characterize is a laboratory creation, this same mutation is found in several natural clusters of H1N1 and H5N1 viruses. Our results demonstrate that, at least in tissue culture, influenza virus receptor-binding activity can be entirely shifted from HA to NA.

Influenza virus expresses two major surface glycoproteins, hemagglutinin (HA) and neuraminidase (NA). The classical view is that HA is a receptor-binding and fusion protein that is essential for viral entry (1), whereas NA is a receptor-cleaving protein that facilitates viral release but is expendable for viral entry (2). Specifically, HA binds to sialic acid on the cell surface, which leads to viral endocytosis and pH-triggered membrane fusion (3), and blocking either HA receptor binding (4) or fusion activity (5–8) neutralizes viral infection. NA promotes the release of newly formed virions by enzymatically cleaving sialic acid from the cell surface—in the absence of NA's sialidase activity, budding virions aggregate on the cell surface due to the binding of HA to cell surface sialic acid (2, 9). Although NA may aid in viral infection *in vivo* by cleaving mucins found in the airways (10), NA activity is completely (2) or nearly completely (11) expendable for viral entry in standard tissue-culture systems.

Although this view of HA as the entry protein and NA as the release protein is almost certainly correct for the vast majority of influenza virus strains, several recent studies have suggested that NA can also acquire receptor-binding activity. In 2010, Lin et al. reported that some recent human H3N2 isolates contained an NA mutation (D151G near the active site) that enables them to bind red blood cells (RBCs) by a mechanism that can be blocked by the NA inhibitor oseltamivir or by anti-NA antibodies (12). Zhu et al. subsequently crystallized an N2 NA with the D151G mutation and showed that this mutant NA could indeed bind with high avidity to some sialylated glycans (13). Gulati et al. reported that oseltamivir blocked the binding to α 2-3-linked sialic acids of human H3N2 isolates with D151G (14). For some of these isolates, oseltamivir also neutralized viral infectivity, suggesting that this mutant NA plays a role in viral entry. However, these viruses still retain the ability to bind to α 2-6-linked sialic acids via HA (14), making it unclear whether NA is the primary receptor-binding protein.

Here we report the discovery of a new mutation (G147R) that enables an N1 NA to completely co-opt the receptor-binding

function normally performed by HA. Viruses with this mutation infect cells in an NA-dependent fashion even after the introduction of multiple mutations and a deletion to highly conserved residues in the HA receptor-binding pocket. We did not isolate the G147R mutation from a naturally occurring virus—rather, it arose *de novo* in a lab-generated chimeric virus during our studies. However, the reported NA sequences of several recent H1N1 and H5N1 isolates do contain G147R. Overall, our study demonstrates the completeness and evolutionary ease with which influenza virus can switch the receptor-binding function between its two glycoproteins.

MATERIALS AND METHODS

Viral strains and genes. All HA sequences were derived from the A/Hong Kong/2/1968 (X-31) H3N2 strain. Mutations to add potential glycosylation sites (Table 1) were first introduced into the parental X-31 HA through site-directed mutagenesis. This HA variant is referred to as “WT” throughout the manuscript. Receptor-binding site mutations (Table 2) were then introduced through site-directed mutagenesis to the WT variant to create the “BindMut HA.” A third variant, “PassMut HA,” also has the additional HA-stalk mutation, K62E in HA2, introduced through site-directed mutagenesis. All NA sequences were derived from the A/WSN/33 (WSN) H1N1 strain. The G147R point mutation was introduced through site-directed mutagenesis. The other viral genes (PB1, PB2, PA, NP, M, and NS) were also from the A/WSN/33 strain. The coding sequences for all HA and NA variants are provided in Table S1 in the supplemental material.

Received 10 July 2013 Accepted 5 September 2013

Published ahead of print 11 September 2013

Address correspondence to Jesse D. Bloom, jlbloom@fhcrc.org.

Supplemental material for this article may be found at <http://dx.doi.org/10.1128/JVI.01889-13>.

Copyright © 2013, American Society for Microbiology. All Rights Reserved.

doi:10.1128/JVI.01889-13

TABLE 1 Sequential and H3 numbering of glycosylation site mutations added to the HA used in this study

Sequential numbering	H3 numbering	Asn residue (sequential/H3)	Glycosylation site change
S61N	S45N	61/45	+
D79N	D63N	79/63	+
T99K	T83K	97/81	-
T138N	T122N	138/122	+
G140S	G124S	138/122	+
T142N	T126N	142/126	+
G151T	G135T	149/133	+
G160N	G144N	160/144	+
G162S	G146S	160/144	+
N264T	N248T	262/246	+

Plasmids. All HA and NA variants generated during the present study were cloned into the bidirectional pHW2000 backbone for reverse-genetics viral rescue (15). The other viral genes were expressed from previously described bidirectional WSN reverse-genetics plasmids (15), which were kindly provided by Robert Webster of St. Jude Children's Research Hospital. For viral rescue experiments, we used a previously described green fluorescent protein (GFP)-based system where the coding region of PB1 is replaced by the coding region of GFP (16). This plasmid is referred to as "PB1flank-eGFP." For some of the experiments, HA and NA were also cloned into an expression plasmid (HDM) which places the gene under the control of a cytomegalovirus (CMV) promoter, followed by an IRES-GFP and the beta-globin poly(A) element.

Cells. Viruses carrying GFP in the PB1 segment were grown in previously described 293T and MDCK-SIAT1 cell lines that constitutively express PB1 under the control of a CMV promoter (16). These cell lines are named 293T-CMV-PB1 and MDCK-SIAT1-CMV-PB1, respectively.

Viral rescue. Cocultures of 293T-CMV-PB1 and MDCK-SIAT1-CMV-PB1 cells were transfected with eight reverse-genetics plasmids encoding PB2, PA, NP, M, NS, HA, NA, and PB1flank-eGFP. Cells were plated at a density of 2×10^5 293T-CMV-PB1 and 0.25×10^5 MDCK-SIAT1-CMV-PB1 cells per well in six-well dishes in D10 (Dulbecco modified Eagle medium supplemented with 10% heat-inactivated fetal bovine serum [FBS], 2 mM L-glutamine, 100 U of penicillin/ml, and 100 μ g of streptomycin/ml). The next day, 250 ng of each plasmid was transfected into the cells using the BioT transfection reagent (Bioland B01-02). At 12 to 18 h posttransfection, the cells were washed with phosphate-buffered saline (PBS), and the medium was changed to influenza growth media (IGM; Opti-MEM supplemented with 0.01% heat-inactivated FBS, 0.3% bovine serum albumin [BSA], 100 U of penicillin/ml, 100 μ g of streptomycin/ml, and 100 μ g of calcium chloride/ml). TPCK (tolylsulfonyl phenylalanyl chloromethyl ketone)-trypsin was added to IGM at 3 μ g/ml immediately before use. Viral supernatants were collected 72 h posttransfection and titered.

Virus titering. The titer of the PB1flank-eGFP viruses was determined by flow cytometry. Briefly, MDCK-SIAT1-CMV-PB1 cells were plated at 10^5 per well in 12-well dishes in IGM and infected 4 h later with 1, 10, or 100 μ l of viral supernatant. At 16 h postinfection, wells with ca. 1 to 10% GFP-positive cells were analyzed by flow cytometry to determine the fraction of cells that were GFP positive. A Poisson equation was used to convert this fraction to the initial multiplicity of infection (MOI), allowing determination of the number of infectious particles in the original inoculum.

HA surface expression. The G1E point mutation in HA2 was introduced into WT and PassMut HA by site-directed mutagenesis, and the mutated genes were cloned into the HDM plasmid. 293T cells were transfected with plasmid encoding each of the HA variants with or without the G1E mutation in triplicate. At 20 h posttransfection, the cells were collected and resuspended in morpholinepropanesulfonic acid (MOPS)-

TABLE 2 Sequential and H3 numbering of receptor-binding site mutations made in BindMut HA

Sequential numbering	H3 numbering	Amino acid change
114	98	Y→F
199	183	H→F
210	194	L→A
237–244	221–228	Deletion

buffered saline (MBS; 15 mM MOPS, 145 mM sodium chloride, 2.7 mM potassium chloride, and 4.0 mM calcium chloride, adjusted to pH 7.4, plus 2% heat-inactivated FBS added immediately before use). Heat-inactivated polyclonal serum from influenza virus-infected mice at a 1:200 dilution was used as the primary antibody to stain for surface HA molecules, and a goat anti-mouse TriColor antibody (Caltag Laboratories catalog no. M32006) at a 1:100 dilution was used as the secondary antibody. Cells were analyzed by flow cytometry to determine the mean fluorescent intensity (MFI) of TriColor (APC channel) among the GFP-positive (transfected) cells. The reported values for each G1E mutant are normalized to the respective wild type.

NA surface expression. A C-terminal V5 epitope tag was added to both WT and G147R NA. Both genes were then cloned into the HDM plasmid and used to transfect 293T cells. At 20 h posttransfection, the cells were collected and stained with an anti-V5 AF647-conjugated antibody (Invitrogen, catalog no. 45-1098) at a 1:200 dilution. Cells were analyzed by flow cytometry to determine the MFI of AF647 (APC channel) among GFP-positive (transfected) cells. Reported values were normalized to the WT NA.

MUNANA activity assay. NA activity was assayed using the fluorogenic 2'-(4-methylumbelliferyl)- α -D-N-acetylneuraminic acid (MUNANA) substrate (Sigma, catalog no. M8639). 293T cells were transfected with HDM plasmid encoding each NA variant in triplicate. At 20 h posttransfection, the cells were collected and diluted 1:40 in a 96-well plate such that each row contained one NA variant. Serial 2-fold dilutions of MUNANA were made across each row of a Costar black flat-bottom 96-well plate. Both plates were prewarmed to 37°C for 20 min. Cells were then quickly resuspended by pipetting and added to the MUNANA plate. Fluorescent readings were taken every minute for 1 h at an excitation wavelength of 360 nm and an emission wavelength of 448 nm. The fluorescence above background was then plotted versus time for each MUNANA concentration to determine the reaction rate. The reaction rate was then plotted against the MUNANA concentration, and the K_m and V_{max} were determined by fitting Michaelis-Menten kinetics curves in GraphPad Prism 5.

Oseltamivir inhibition assay. 293T cells were transfected with HDM plasmids encoding WT and G147R NA in triplicate. At 20 h posttransfection, the cells were collected, diluted, and then incubated with decreasing concentrations of oseltamivir carboxylate (kindly provided by Roche) at 37°C for 30 min to allow for oseltamivir binding. MUNANA was added to 300 μ M, and incubation continued for 45 min. The reaction was quenched by adding a solution of 0.153 M NaOH in 81.5% ethanol, and the signal was read as described above. Values were normalized to a no-oseltamivir control for each NA variant to determine the percent remaining activity.

Mouse infections. Serum for neutralization assays, hemagglutination inhibition assays, and cell surface staining was obtained from influenza virus-infected mice. Mice were intranasally infected with replication-competent virus after being anesthetized with 2 mg of ketamine and 0.2 mg of xylazine per mouse. At 3 weeks postinfection, a booster infection was done using the same protocol. Mice were then euthanized and bled by cardiac puncture 4 weeks after initial infection or 1 week after the booster. For neutralization assays, mouse serum was heat inactivated at 56°C for 40 min prior to use. For hemagglutination inhibition assays, serum was heat inactivated, and then antibodies were purified by using a protein A col-

TABLE 3 N1 sequences with R at position 147 (N2 numbering)

GenBank accession no.	Strain	Lineage
ABD78030	A/South_Canterbury/59/2000	Seasonal H1N1
ABX58495	A/Tennessee/UR06-0238/2007	Seasonal H1N1
ACY01424	A/Hamedan/117/2007	Seasonal H1N1
ACA33659	A/Texas/74/2007	Seasonal H1N1
ADZ53071	A/Hong_Kong/01045/2008	Seasonal H1N1
ADP89151	A/Thailand/Siriraj-01/2008	Seasonal H1N1
ADP89152	A/Thailand/Siriraj-02/2008	Seasonal H1N1
ADP89155	A/Thailand/Siriraj-05/2008	Seasonal H1N1
ACM17331	A/Austria/404811/2008	Seasonal H1N1
ADA69512	A/Austria/404821/2008	Seasonal H1N1
ADA69518	A/Austria/405179/2008	Seasonal H1N1
ACI94940	A/Austria/406109/2008	Seasonal H1N1
BAH22142	A/Yokohama/30/2008	Seasonal H1N1
ACM90850	A/Johannesburg/279/2008	Seasonal H1N1
ADZ53099	A/Hong_Kong/17566/2009	Seasonal H1N1
ADC45782	A/Niigata/08F188/2009	Seasonal H1N1
AET84319	A/Iraq/WRAIR1683P/2009	Seasonal H1N1
ADA71159	A/Novosibirsk/3/2009	Seasonal H1N1
ACU44027	A/Kentucky/08/2009	Seasonal H1N1
ACU44235	A/Kentucky/08/2009	Seasonal H1N1
ADN26074	A/Finland/614/2009	Pandemic H1N1
AFE11259	A/Tianjinhedong/SWL44/2011	Pandemic H1N1
AFN20030	A/Singapore/SGH02/2011	Pandemic H1N1
ADG59204	A/chicken/Anhui/39/2004	Avian H5N1
ADG59211	A/chicken/Gansu/44/2004	Avian H5N1
ADB26210	A/chicken/Nigeria/08RS848-93/2007	Avian H5N1
AFH53768	A/chicken/Egypt/Kalyobia-18-CLEVB/2011	Avian H5N1
AGG52920	A/chicken/Bangladesh/12VIR-7140-1/2011	Avian H5N1
AGG52921	A/chicken/Bangladesh/12VIR-7140-2/2012	Avian H5N1
AGG52922	A/chicken/Bangladesh/12VIR-7140-3/2012	Avian H5N1
AGG52925	A/chicken/Bangladesh/12VIR-7140-6/2012	Avian H5N1

umn (Thermo Scientific, catalog no. 89952) and concentrated to the original volume prior to use. This animal work was approved under FHCRC IACUC protocol 1893.

Neutralization assays. Neutralization assays were performed using the PB1flank-eGFP viruses. To reduce the background medium autofluorescence in the GFP channel, we developed a neutralization assay medium (NAM) consisting of Medium 199 supplemented with 0.01% heat-inactivated FBS, 0.3% BSA, 100 U of penicillin/ml, 100 µg of streptomycin/ml, 100 µg of calcium chloride/ml, and 25 mM HEPES. Polyclonal serum or oseltamivir was diluted down the columns of a 96-well plate in NAM, and virus was added at an MOI that ranged from 0.1 to 0.8 for the different viruses. Plates were incubated at 37°C for 1 h to allow oseltamivir or antibody binding, and then 4×10^4 MDCK-SIAT1-CMV-PB1 cells were added per well. A no-serum or no-oseltamivir control row for each virus was included to give a maximum infectivity value, and a no-virus control row was included to give the background fluorescence. After an 18-h incubation, GFP fluorescence intensity was measured using an excitation wavelength of 485 nm and an emission wavelength of 515 nm (12-nm slit widths). The signal above background for each well was normalized to its respective no-oseltamivir or no-serum control; values are reported as percent infectivity remaining averaged over triplicate measurements.

Hemagglutination inhibition assays. Hemagglutination inhibition assays were performed using turkey (Lampire Biological Laboratories, catalog no. 7249409), chicken (Innovative Research, catalog no. IC05-0810), or guinea pig (Innovative Research, catalog no. IC05-0910) RBCs diluted to 0.5% in PBS. The hemagglutination titer for each virus and blood cell type was determined, and then 8 HAU used for inhibition

assays. Next, 10 µl containing 8 HAU of virus was preincubated at 37°C with 40 µl of serum or oseltamivir for 1 h in U-bottom plates, and then 50 µl of RBCs were added. Plates were scored after 1 h of incubation at room temperature.

VLP production. To produce virus-like particles (VLPs) expressing NA but not HA on their surfaces, 293T cells in D10 were transfected with an HDM plasmid expressing M1 and M2 from the A/PR/8/34 (H1N1) strain separated by a T2A linker and an HDM plasmid expressing either WT or G147R NA. The medium was changed to IGM at 24 h posttransfection, and the VLP supernatant was collected at 72 h posttransfection. Supernatants were clarified at $2,000 \times g$ for 5 min to pellet cell debris. The clarified supernatant was then concentrated with a 100-kDa cutoff centrifugal concentrator. The MUNANA activity of the collected VLPs was determined for equal volumes of concentrated supernatants.

Viral growth in the presence of RDE. MDCK-SIAT1-CMV-PB1 cells were plated in six-well dishes at a density of 5×10^4 cells per well in D10. After 18 h, the medium was changed to IGM with 4 µg of TPCK-trypsin/ml after a PBS wash. Half of the wells also contained the bacterial sialidase RDE (Sigma, catalog no. C8772; one vial resuspended in 5 ml of sterile water) added at 5 µl/ml. Plates were incubated at 37°C for 1 h to allow for RDE cleavage, and then infected at an MOI of 0.05. Beginning at 36 h postinfection, the supernatant was collected and titered every 12 h as previously described.

Analysis of G147R mutation in naturally occurring sequences. To examine the occurrence of G147R in naturally occurring sequences, we downloaded all N1 protein sequences in the Influenza Virus Resource (17) as of 3 July 2013. These sequences were pairwise aligned with the WSN G147R NA to identify all sequences with an R at position 147 (these sequences are listed in Table 3). To examine whether the sequences with G147R formed phylogenetic clusters, an initial tree was built using RAxML (18) on all G147R sequences and a subset of the other sequences. Based on visual inspection of this tree, three different clusters of at least three G147R sequences were identified. Comprehensive phylogenetic trees of sequences with high identity to these apparent clusters were then built using BEAST (19) with date-stamped sequences using the JTT (20) model of substitution. Maximum clade credibility trees were computed and visualized using FigTree to give the images shown in Fig. 8.

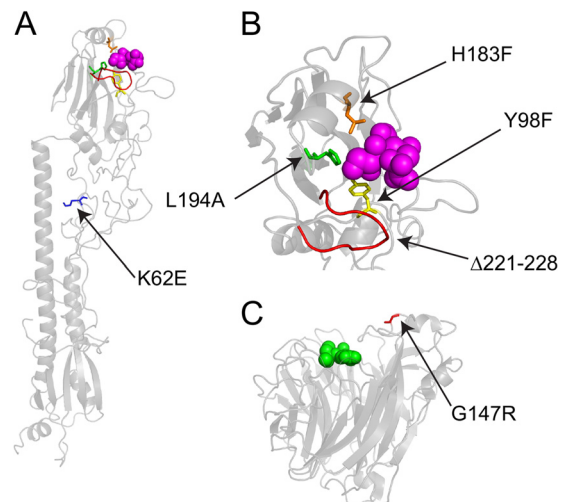


FIG 1 Attempted growth of a virus with extensive mutations in the HA receptor-binding pocket selects for a mutation near the active site of NA. (A) Crystal structure (PDB 4HMG) of an HA monomer with a sialic acid analogue (purple spheres) bound in the receptor-binding pocket. The sites of the binding-pocket mutations are shown in colors other than gray, and the site of stalk mutation K62E in HA2 is also indicated. (B) Zoomed-in image of the receptor-binding pocket of the HA structure shown in panel A. (C) Crystal structure (PDB 2HU4) of an NA monomer with oseltamivir (green spheres) in the active site and the site of the passage-derived G147R mutation shown in red.

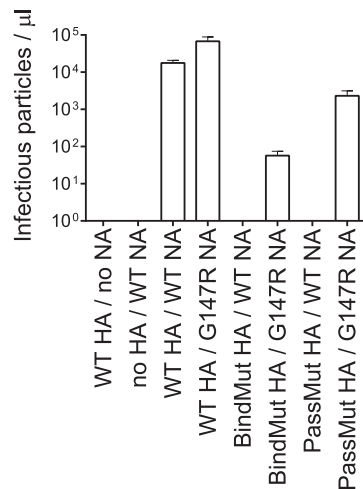


FIG 2 Viruses with the HA receptor-binding mutations can only be rescued with the mutant G147R NA. Shown are virus titers in the supernatant 72 h after attempted rescue of the indicated viruses by reverse genetics. Virus containing the BindMut HA can only be rescued in combination with the G147R NA. Further passage of this BindMut HA/G147R NA virus selected for the additional K62E mutation in HA2. The PassMut HA (which contains this HA2 mutation) also can only be rescued in combination with the G147R NA. The means and standard errors for three replicates are shown.

RESULTS

Loss of HA receptor-binding is compensated by a mutation in NA. We created a mutant of the HA from the A/Hong Kong/2/1968 (H3N2) strain that we expected to be unable to bind to its sialic acid receptor. This mutant contained three point mutations previously shown to individually nearly abolish HA receptor binding (21) and a loop deletion near the receptor-binding pocket (22). In the H3 numbering scheme, these mutations are Y98F, H183F, and L194A and the deletion of amino acids 221 to 228 (Fig. 1A and B; Table 2). We also added seven N-linked glycosylation site motifs at positions where glycosylation is found in contemporary human H3N2 HAs (potentially glycosylated asparagines at residues 45, 63, 122, 126, 133, 144, and 246 in H3 numbering; Table 1), since glycosylation of HA has been shown to reduce receptor avidity (23). This presumed binding-deficient mutant HA is henceforth referred to as BindMut HA.

The BindMut HA was used as a negative control during rescue of viruses by reverse genetics (16) for a series of other experiments. We did not expect to see growth of virus containing the BindMut HA due to its presumed lack of receptor-binding ability. To our surprise, in one rare instance we isolated a virus with the BindMut HA that grew to moderate titers in tissue culture. The isolated virus contained the BindMut HA and all of the other genes from the A/WSN/33 (H1N1) strain. We sequenced this isolate and found no mutations or reversions in HA, but one point mutation, G147R (N2 numbering), was identified in NA. This mutation is located somewhat above the NA active site in the NA crystal structure (Fig. 1C). Further passage of the virus yielded a variant that grew to increased titers. This virus had retained the G147R NA mutation and had also acquired a stalk mutation, K62E in HA2 (H3 numbering) (Fig. 1A). This HA mutant, which contains all of the original receptor-binding site mutations and glycosylation sites plus the K62E stalk mutation, is henceforth referred to as PassMut HA (for passage mutant HA).

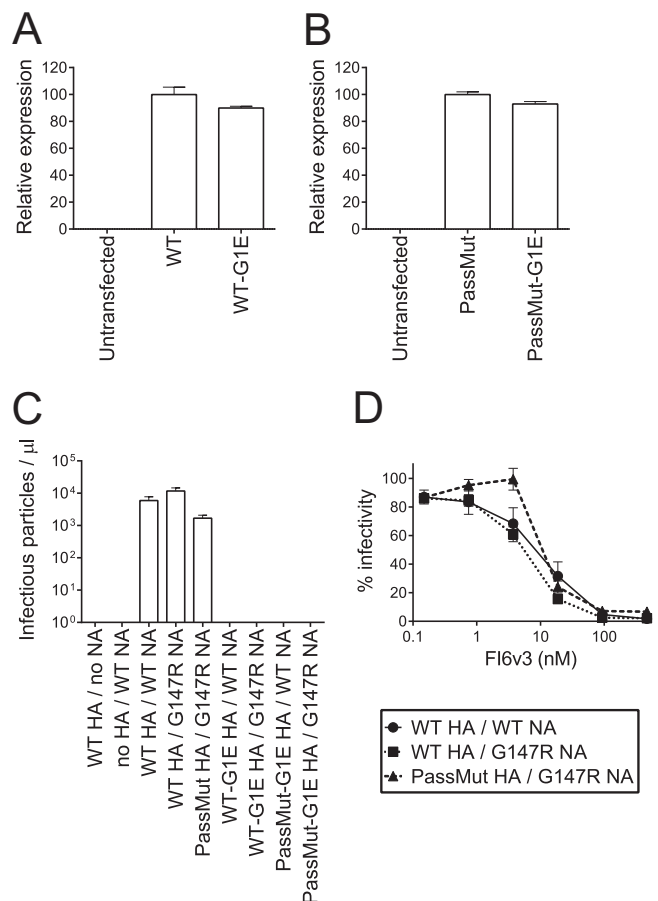


FIG 3 HA is still required for viral membrane fusion. (A) Introduction of the fusion-blocking G1E mutation into WT HA does not substantially impact HA surface expression, as quantified by antibody staining and flow cytometry of transfected 293T cells. (B) Introduction of the G1E mutation into PassMut HA also does not substantially impact HA surface expression. (C) G1E completely blocks the rescue of infectious virus by reverse genetics, regardless of the NA used. Shown are the virus titers in the supernatant 70 h after attempted rescue of the indicated viruses by reverse genetics. (D) The infectivity of all viral variants is neutralized by the fusion-inhibiting antibody FI6v3, regardless of which glycoprotein they use to bind to the receptor. In all panels, the data represent the means and standard errors of three replicates.

To determine whether the HA and NA mutations were responsible for the growth phenotypes observed, we created reverse-genetics plasmids for all HA and NA variants. Three HA variants were made: a variant we will term wild-type (WT) HA, which has the seven glycosylation sites added but none of the receptor-binding site mutations, the BindMut HA, and the PassMut HA. Two NA variants were created: wild-type A/WSN/33 NA (WT NA) and WSN NA with the G147R mutation (G147R NA). We then attempted to rescue viruses containing all combinations of these HAs and NAs in the WSN background.

As expected, we were able to efficiently rescue virus carrying the WT HA paired with either WT or G147R NA (Fig. 2). Also as expected, we were unable to rescue virus when the presumed binding-deficient BindMut or PassMut HAs were paired with WT NA. However, we could rescue moderate levels of virus carrying the BindMut HA and G147R NA, suggesting that G147R compensated for the loss of HA receptor binding. Virus containing the

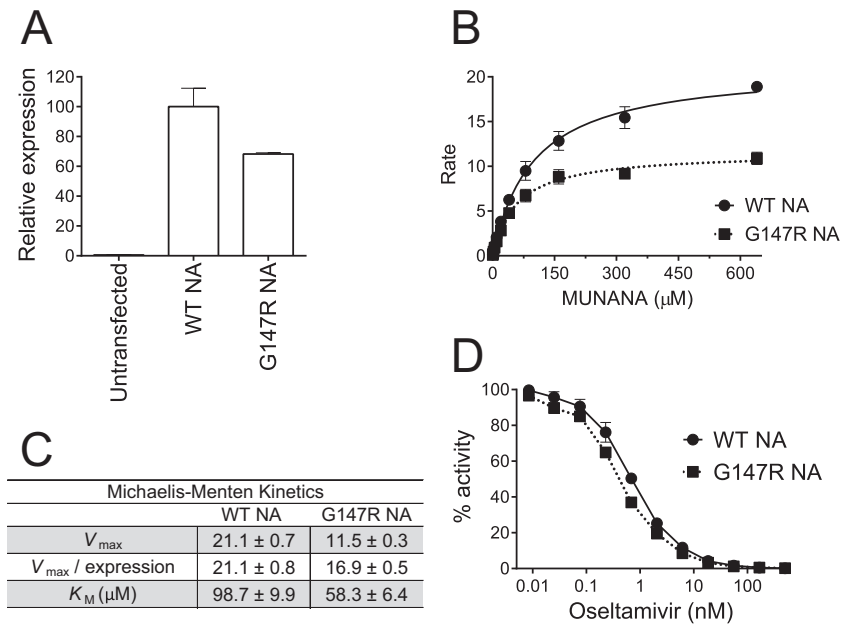


FIG 4 The G147R NA is an active sialidase that is inhibited by oseltamivir. (A) Surface expression of WT and G147R NA with C-terminal V5 epitope tags in transfected 293T cells. Expression of G147R NA is ca. 70% that of WT. (B) Rate of MUNANA cleavage at increasing substrate concentrations. Michaelis-Menten kinetics curves were fit to determine the K_M and V_{max} . (C) Enzyme kinetics for WT and G147R NA. V_{max} is also normalized to expression levels in panel A to give a value proportional to k_{cat} . (D) NA activity at increasing concentrations of oseltamivir. Both NAs are inhibited at similar concentrations. The y axis shows the percent remaining activity relative to the same NA variant in the absence of oseltamivir. For all panels, data represent the means and standard errors of three replicates.

PassMut HA and G147R NA grew to levels nearly as high as that of virus with the WT HA and WT NA. These results led us to hypothesize that the G147R mutation had enabled NA to acquire the receptor-binding function normally performed by HA.

HA is still required for viral fusion. Although we hypothesized that NA was functioning as the receptor-binding protein in our mutant viruses, we wanted to determine whether HA was still needed to mediate membrane fusion. To test this, we introduced a point mutation that has been shown to abolish the fusion activity of HA, G1E in HA2 (24). The G1E mutation was introduced into both the WT and PassMut HA. To confirm that G1E did not affect HA levels at the cell surface, we used cell surface staining with polyclonal anti-HA serum and flow cytometry to quantify cell surface protein levels. Sera from mice infected with WT HA virus were used to stain WT- and WT-G1E-expressing cells, while serum from mice infected with PassMut HA virus was used to stain PassMut- and PassMut-G1E-expressing cells. In both cases, expression of the G1E mutant was $>90\%$ that of the matched parent HA (Fig. 3A and B), indicating that G1E does not substantially impair HA folding or trafficking to the cell surface. We then attempted to rescue virus containing the G1E HAs with either WT or G147R NA. We were unable to rescue any G1E-containing viruses, indicating that abolishing HA's fusion function ablates viral growth (Fig. 3C).

To further confirm the requirement for HA-mediated fusion, we performed neutralization assays with the anti-fusion antibody FI6v3 (25). This broadly neutralizing antibody locks HA into the prefusion conformation. All viruses were neutralized by FI6v3 at similar concentrations, regardless of their HA and NA composition (Fig. 3D). Taken together, these data show that HA is required for fusion regardless of whether or not the virus has NA with the G147R mutation.

G147R NA is still an active sialidase that is expressed at the cell surface. We next tested whether G147R altered NA's surface expression or enzymatic activity as a sialidase. To assay for NA surface expression, a C-terminal V5 tag was added to both the WT and G147R variants, and then 293T cells were transfected and surface stained for flow cytometry. G147R NA was found to be expressed on the cell surface at 70% the level of WT NA (Fig. 4A).

We then measured the kinetics of cleavage of the NA surrogate substrate MUNANA by 293T cells transfected with both NA variants (Fig. 4B and C). The maximum reaction rate, V_{max} , for G147R NA was ca. 55% that of WT NA, but when normalized to account for G147R's lower surface expression, the reduction in G147R NA's per-enzyme catalytic rate is only ca. 20%. G147R had a ~ 2 -fold-higher substrate affinity than WT, as indicated by a 2-fold-lower K_M . Although these enzymatic parameters are not identical, the differences are sufficiently small that they seem unlikely to fully explain G147R's dramatic acquisition of the capability to serve as the primary receptor-binding protein. However, it is important to note that our assays were performed using the single surrogate substrate MUNANA, and the results may not be representative of NA's binding and cleavage of all possible sialic-acid variants. It is possible that the cells express some other sialic acid structure that is bound by the G147R NA but is cleaved with much slower kinetics than those observed for the MUNANA substrate.

Oseltamivir and anti-NA antibodies inhibit infection and hemagglutination by viruses dependent on the G147R NA. We next tested the ability of oseltamivir to inhibit enzyme activity for both the WT and G147R NA (Fig. 4D). Both variants were inhibited by oseltamivir at similar concentrations, indicating that oseltamivir can still bind to the active site of the G147R NA. We therefore decided to test whether oseltamivir could also inhibit the receptor binding of viruses dependent on the G147R NA.

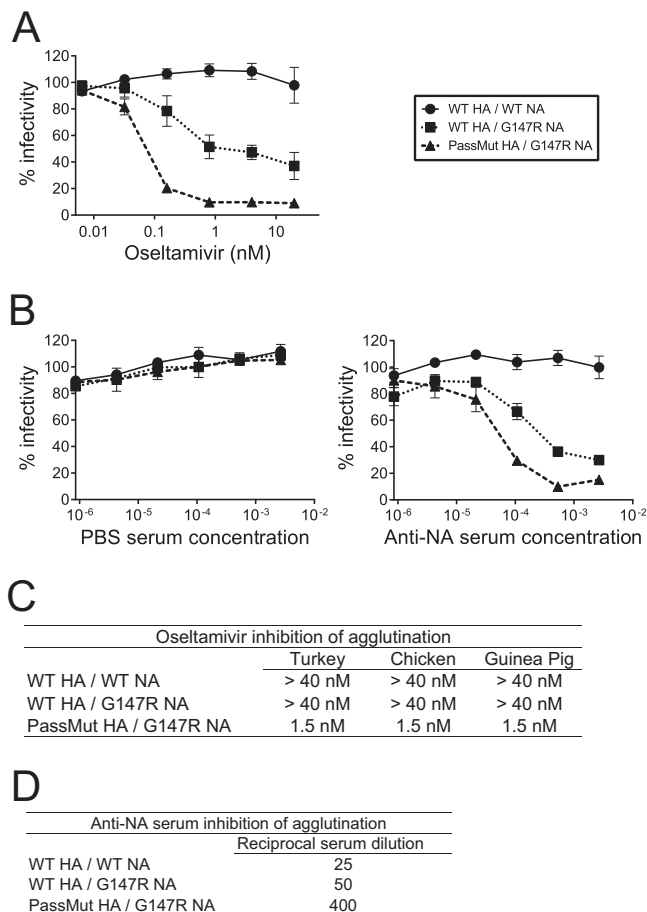


FIG 5 Osetamivir neutralizes and inhibits hemagglutination by viruses that utilize G147R NA as the receptor-binding protein. (A) The extent of virus neutralization by osetamivir depends on the degree to which NA is utilized as the receptor-binding protein. PassMut HA/G147R NA uses NA as the receptor-binding protein and is nearly completely neutralized by osetamivir. WT HA/G147R NA uses both HA and NA as receptor-binding proteins and is partially neutralized by osetamivir. WT HA/WT NA uses HA as the receptor-binding protein and is resistant to neutralization by osetamivir. (B) Effects similar to those described in panel A are seen when viral infectivity is inhibited with polyclonal anti-NA antibodies from mouse serum. The plots show neutralization by serum from mice infected with virus carrying the G147R NA, or mock infected with PBS. Both panels A and B represent the means and standard errors of three replicates. (C) The agglutination of RBCs by PassMut HA/G147R NA is inhibited by osetamivir while WT HA/WT NA and WT HA/G147R NA are resistant to inhibition at all concentrations tested. RBCs from the indicated species were incubated with 8 HA units of virus pretreated with the indicated amounts of osetamivir. (D) Agglutination of turkey RBCs by PassMut HA/G147R NA is inhibited at low concentrations of polyclonal anti-NA antibodies from mouse serum. WT HA/WT NA and WT HA/G147R NA are much more resistant to inhibition. Values are reported as the reciprocal of the dilution factor for which complete inhibition was seen.

We tested osetamivir's ability to block infectivity of three viruses: WT HA/WT NA, WT HA/G147R NA, and PassMut HA/G147R NA (Fig. 5A). WT HA/WT NA virus was uninhibited at all concentrations tested, a finding consistent with the prevailing belief that NA activity is not crucial for viral entry (2). However, PassMut HA/G147R NA was strongly neutralized at low nanomolar osetamivir concentrations, which is consistent with the hypothesis that NA is the viral attachment protein for this virus. WT HA/G147R NA showed an intermediate phenotype, likely because

oseltamivir inhibits NA-mediated but not HA-mediated receptor binding by this virus.

We also tested whether polyclonal mouse serum with NA-specific antibodies could block infectivity. Sera were obtained from mice infected with a virus containing G147R NA, but with an H1 subtype HA. Because the WT and G147R NAs differ at only a single site, this polyclonal serum should substantially react with both NAs but should not recognize the H3 subtype HA present in all three viruses tested. The degree of neutralization of the three viruses by this serum was similar to that seen for osetamivir (Fig. 5B). PassMut HA/G147R NA was strongly neutralized, WT HA/WT NA was completely uninhibited, and WT HA/G147R NA showed an intermediate phenotype.

To directly test whether osetamivir blocks viral attachment to cells, we performed hemagglutination inhibition assays. All RBC types tested (turkey, chicken, and guinea pig) were effectively agglutinated by the PassMut HA/G147R NA virus, but in all cases this agglutination was inhibited down to an osetamivir concentration of 1.5 nM. In contrast, the WT HA/WT NA and WT HA/G147R NA were uninhibited at all of the osetamivir concentrations tested (Fig. 5C).

A hemagglutination inhibition assay was also performed in the presence of purified polyclonal anti-NA antibodies from mouse serum. PassMut HA/G147R NA was potently inhibited, whereas WT HA/WT NA and WT HA/G147R NA were much more resistant (Fig. 5D). Taken together, these data show that infectivity and cell binding of the PassMut HA/G147R NA virus are inhibited by blocking NA with either a small molecule inhibitor or polyclonal antibodies. These results strongly suggest that the PassMut HA/G147R NA viruses are using NA as the sole receptor-binding protein.

NA-only VLPs can agglutinate RBCs, and agglutination is reversibly blocked by osetamivir. To conclusively show that the cell binding of PassMut HA/G147R NA is completely independent of HA, we produced VLPs that expressed NA but no HA. We did this by transfecting 293T cells with plasmids expressing M1 and M2 and either WT or G147R NA, since NA alone has previously been shown to be sufficient for VLP production with M1 slightly enhancing VLP release (26), and M2 is known to promote membrane scission (27). The total NA activity in the G147R VLP supernatant was 77% that of WT NA VLP supernatant, a finding consistent with the slightly reduced activity of G147R NA reported in Fig. 4.

We used concentrated VLP supernatants to perform a hemagglutination assay with turkey RBCs. Figure 6A shows images of the assay taken every 20 min. The WT NA-only VLPs slightly increased the speed of RBC settling relative to the PBS control, suggesting that removal of cell surface sialic acid might promote the settling of RBCs, possibly by removing negative charges from the cell surface. At high concentrations, the G147R NA-only VLPs initially slightly agglutinated the RBCs, but this agglutination soon disappeared, and the RBCs settled to the bottom of the plate. However, at moderate concentrations, the G147R NA-only VLPs potently agglutinated the RBCs over the full 60-min time course. After 60 min, we added osetamivir to all wells at a high concentration. Osetamivir reversed the agglutination by the G147R VLPs; this observation is consistent with the idea that osetamivir can elute the VLPs off the RBCs by competitively binding to the G147R NA.

Overall, the results in Fig. 6A show that the G147R NA can bind VLPs to RBCs in a reversible manner. The eventual disappearance

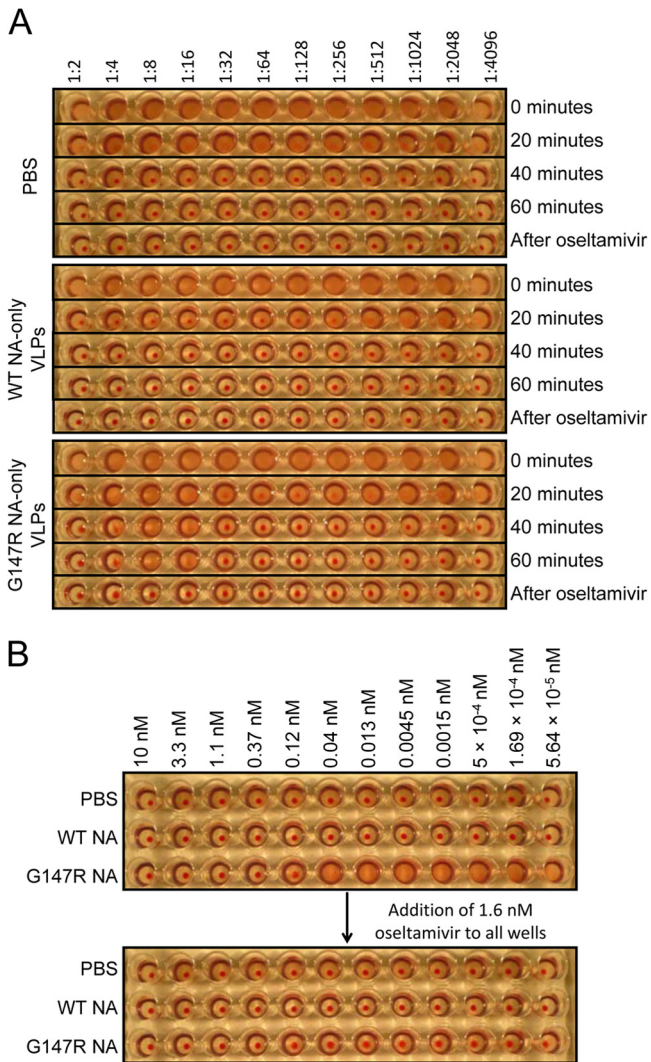


FIG 6 G147R NA-only VLPs agglutinate RBCs, and agglutination is inhibited by oseltamivir. (A) A hemagglutination assay was performed using WT and G147R NA VLPs. VLPs were serially diluted 2-fold across a U-bottom plate, turkey RBCs were added, and the plate was imaged every 20 min. At 60 min, oseltamivir was added to all wells to a final concentration of 10 nM. The plate was imaged again 20 min later by which time agglutination by G147R VLPs had been reversed. (B) A hemagglutination inhibition assay was performed using serial 3-fold dilutions of oseltamivir across a U-bottom plate. VLPs from HA assay were added at a concentration corresponding to the 1:8 dilution in panel A. The plate was imaged 60 min after the addition of turkey RBCs. Oseltamivir was then added to all wells at a final concentration of 1.6 nM, and the plate was imaged 20 min later.

of agglutination at high G147R NA-only VLP concentrations suggests that G147R NA might slowly cleave the same receptor to which it initially binds. In this scenario, at high VLP concentrations the G147R NA eventually removes all of the receptor, making the RBCs resistant to continued agglutination. At moderate VLP concentrations, the rate of receptor removal is lower and so long-term agglutination is observed.

We next performed a hemagglutination inhibition assay in the presence of increasing dilutions of oseltamivir and a G147R NA-only VLP concentration that caused long-term agglutination. Oseltamivir inhibited agglutination by the G147R NA-only VLPs

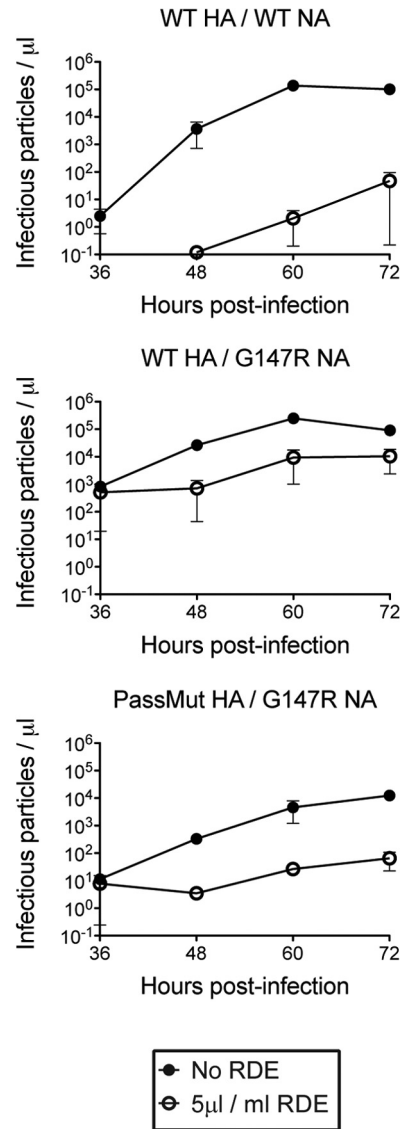


FIG 7 Treatment with an exogenous bacterial sialidase (receptor-destroying enzyme [RDE]) only partially inhibits infection by receptor-binding NA viruses. Cells both with or without RDE pretreatment were infected with each viral variant at an MOI of 0.05. The supernatant was collected every 12 h postinfection, and virus titers were determined. The data represent the means and standard errors of three replicates.

down to concentrations of 0.12 nM. At lower oseltamivir concentrations, agglutination did occur, but it could again be reversed by the addition of high concentrations of oseltamivir after 1 h (Fig. 6B). Taken together, these data show that G147R NA is sufficient for agglutination in the complete absence of HA.

Sialidase treatment only partially inhibits infection by G147R NA viruses. We wanted to determine whether the G147R mutant NA still binds to the canonical sialic-acid receptor recognized by HA. To test this, cells were pretreated with a broad-spectrum bacterial sialidase (receptor-destroying enzyme [RDE]) for 1 h and then infected with WT HA/WT NA, WT HA/G147R NA, and PassMut HA/G147R NA viruses at an MOI of 0.05. The viral supernatant was titered every 12 h beginning at 36 h postinfection. RDE treatment nearly completely inhibited growth of WT

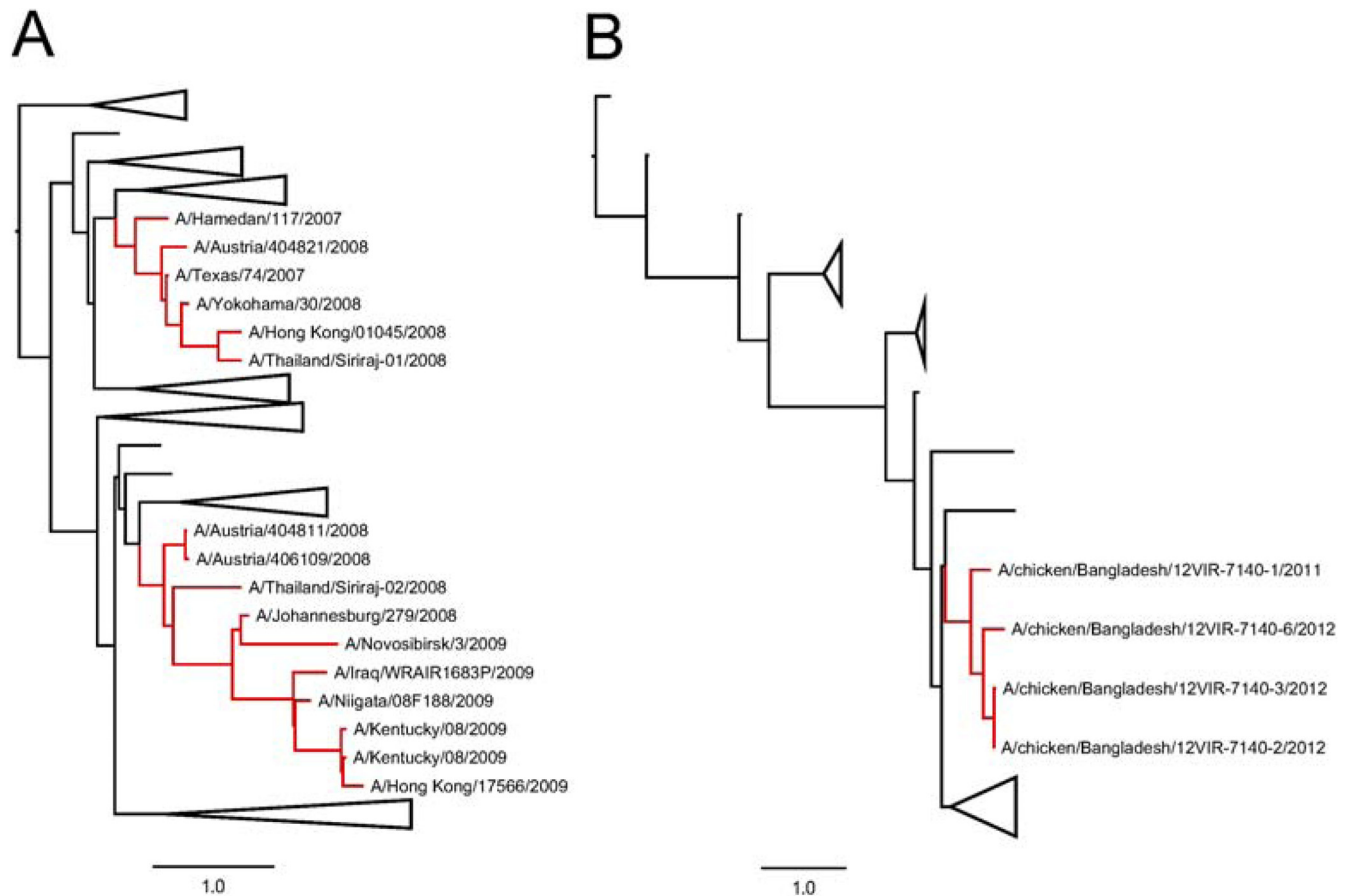


FIG 8 There are several phylogenetic clusters of N1 NA sequences containing G147R, suggesting that this mutation arose during natural evolution rather than as a laboratory artifact. (A) There are two clusters of sequences with G147R in human seasonal H1N1. (B) There is one cluster of sequences with G147R in chicken H5N1. In both trees, sequences with G147R have branches colored red and strain names shown, while sequences without G147R have branches colored black and lack sequence names. Clades without G147R are collapsed into triangles to shrink the sizes of the trees for visual display. Scale bars indicate a length equal to 1 year. In panel A, there are two strains named A/Kentucky/08/2009 since there are two sequence variants for this strain in the Influenza Virus Resource.

HA/WT NA except for low levels of viral growth at late time points (Fig. 7). However, the WT HA/G147R NA and PassMut HA/G147R NA viruses were substantially less inhibited by RDE treatment of the cells (Fig. 7), although their growth was still clearly reduced. These results suggest that the receptor for the G147R NA is more refractory to RDE cleavage than the receptor for HA. However, we were unable to ascertain whether the G147R NA recognizes a non-sialic-acid receptor or simply recognizes a class of sialic acid moieties that is partially resistant to RDE cleavage since we lack a way to independently assess the extent to which all sialic acid has been removed by RDE. It seems quite plausible that G147R could recognize a sialic acid structure that is incompletely removed by RDE.

G147R NA mutation is present in some naturally occurring N1 isolates. To determine whether G147R is present in naturally occurring influenza virus isolates, we examined all 19,528 N1 NA protein sequences in the Influenza Virus Resource (17) with an unambiguous identity at position 147. The vast majority of these sequences contain a G at position 147. However, 31 sequences contain the G147R mutation, and 24 contain the G147E mutation at this site. Table 3 gives a complete list of the sequences with G147R and their lineage. The majority of these sequences are from the human seasonal H1N1 lineage that circulated prior to the 2009

pandemic, but there are also several sequences from the 2009 swine-origin pandemic H1N1 lineage and several from avian H5N1 lineages. All of these sequences have isolation dates after the year 2007 with the exception of one isolate from 2000 and two isolates from 2004.

We have no direct way to determine whether G147R was actually present in circulating viruses, whether it arose during tissue-culture adaptation prior to sequencing, or whether it was the result of a sequencing error. However, a phylogenetic analysis strongly suggests that a substantial number of the G147R sequences reflect the actual natural occurrence of this mutation. Specifically, as shown in Fig. 8, there are two human seasonal H1N1 and one chicken H5N1 phylogenetic cluster of four or more sequences containing G147R. Since laboratory artifacts would likely occur fairly randomly among sequenced isolates, the existence of these phylogenetic clusters provides strong circumstantial evidence that G147R has arisen naturally in N1 NAs several times during influenza's evolution.

DISCUSSION

We have described a surprising influenza virus mutant in which an N1 NA serves as the receptor-binding protein, enabling the virus to grow to high titers in the absence of HA receptor-binding

function. HA is traditionally viewed as possessing two highly conserved functions: receptor binding and membrane fusion. Although HA is still needed for fusion in our mutant viruses, it is remarkable to consider the evolutionary ease with which NA was able to co-opt the receptor-binding properties normally associated with HA. Specifically, the single amino acid substitution G147R allows NA to mediate viral infection and RBC agglutination in a manner that can be reversibly blocked by NA inhibitors and anti-NA antibodies.

Also surprisingly, the mutant G147R NA is still active as a sialidase with kinetics that are not dramatically different than those of the wild-type parental NA, at least on the single surrogate substrate for which we were able to obtain enzymatic parameters. Of course, it remains quite possible that the G147R NA binds but fails to cleave (or only cleaves very slowly) some other sialic acid structure found on the cell surface. However, even in this case, our results show that it is possible for NA to evolve receptor-binding properties without completely sacrificing its sialidase activity.

Our results were unexpected because the receptor-binding and receptor-cleaving activities of influenza virus A are typically fully segregated between HA and NA. However, several other viruses that use sialic acid as a receptor combine these activities within a single protein. For example, the single hemagglutinin-neuraminidase of human parainfluenza virus both binds and cleaves sialic acid in a balanced fashion that enables effective viral infection and propagation (28). Similarly, the single hemagglutinin-esterase protein of influenza virus C binds to a sialic acid structure that is then modified to a nonbindable form via the protein's esterase activity (29). Our findings indicate that a relatively small number of mutations are sufficient to allow influenza virus A to similarly combine the receptor-binding and receptor-destroying activities within NA, at least in tissue culture settings.

The mutant G147R NA that we have described arose *de novo* during our experiments in the background of the NA from the lab-adapted WSN influenza virus strain and was characterized in the context of a lab-generated chimeric virus. However, this same mutation is found in several natural clusters of human H1N1 and chicken H5N1 sequences, indicating that it also has arisen several times during natural evolution.

Our results are especially noteworthy because they come on the heels of several recent studies describing how a single mutation (D151G) has conferred receptor-binding activity on the NAs of some recent human H3N2 strains (12–14). It is possible that both the mutation that we have described and D151G are evolutionary oddities, with no real implications for influenza more generally. However, given that the properties of both these mutations were only discovered by happenstance years after they began to appear in circulating influenza virus isolates, it is also worth considering that they might be indicative of an underappreciated aspect of influenza virus biology. If receptor-binding NA variants turn out to be common, it would be interesting to examine their implications for influenza virus transmission, pathogenesis, and the effectiveness of humoral immunity that is typically envisioned as blocking HA-mediated attachment of viruses to target cells.

ACKNOWLEDGMENTS

We thank Roche for providing the oseltamivir carboxylate, Laura Austin for assistance with initiating some of the experiments, Alex Balazs for providing the genes for Fl6v3, Colin Correnti and Roland Strong for purification of the Fl6v3 antibody, and the FHCRC Flow Cytometry facility.

The research reported here was supported by grants from the NIAID and NIGMS of the National Institutes of Health under awards R01GM102198 and K22AI093789 and NRSA training grant T32GM07270 (K.A.H.).

The content is solely the responsibility of the authors and does not necessarily represent the official views of the National Institutes of Health.

REFERENCES

1. Skehel JJ, Wiley DC. 2000. Receptor binding and membrane fusion in virus entry: the influenza hemagglutinin. *Annu. Rev. Biochem.* 69:531–569.
2. Liu C, Eichelberger MC, Compans RW, Air GM. 1995. Influenza type A virus neuraminidase does not play a role in viral entry, replication, assembly, or budding. *J. Virol.* 69:1099–1106.
3. Skehel JJ, Bayley PM, Brown EB, Martin SR, Waterfield MD, White JM, Wilson IA, Wiley DC. 1982. Changes in the conformation of influenza virus hemagglutinin at the pH optimum of virus-mediated membrane fusion. *Proc. Natl. Acad. Sci. U. S. A.* 79:968–972.
4. Jones JC, Turpin EA, Bultmann H, Brandt CR, Schultz-Cherry S. 2006. Inhibition of influenza virus infection by a novel antiviral peptide that targets viral attachment to cells. *J. Virol.* 80:11960–11967.
5. Okuno Y, Isegawa Y, Sasao F, Ueda S. 1993. A common neutralizing epitope conserved between the hemagglutinins of influenza A virus H1 and H2 strains. *J. Virol.* 67:2552–2558.
6. Ekiert DC, Bhabha G, Elsliger MA, Friesen RH, Jongeneelen M, Throbsby M, Goudsmit J, Wilson IA. 2009. Antibody recognition of a highly conserved influenza virus epitope. *Science* 324:246–251.
7. Sui J, Hwang WC, Perez S, Wei G, Aird D, Chen LM, Santelli E, Stec B, Cadwell G, Ali M, Wan H, Murakami A, Yammanuru A, Han T, Cox NJ, Bankston LA, Donis RO, Liddington RC, Marasco WA. 2009. Structural and functional bases for broad-spectrum neutralization of avian and human influenza A viruses. *Nat. Struct. Mol. Biol.* 16:265–273.
8. Boriskin YS, Leneva IA, Pecheur EI, Polyak SJ. 2008. Arbidol: a broad-spectrum antiviral compound that blocks viral fusion. *Curr. Med. Chem.* 15:997–1005.
9. Palese P, Tobita K, Ueda M, Compans RW. 1974. Characterization of temperature sensitive influenza virus mutants defective in neuraminidase. *Virology* 61:397–410.
10. Matrosovich MN, Matrosovich TY, Gray T, Roberts NA, Klenk HD. 2004. Neuraminidase is important for the initiation of influenza virus infection in human airway epithelium. *J. Virol.* 78:12665–12667.
11. Ohuchi M, Asaoka N, Sakai T, Ohuchi R. 2006. Roles of neuraminidase in the initial stage of influenza virus infection. *Microbes Infect. Inst. Pasteur* 8:1287–1293.
12. Lin YP, Gregory V, Collins P, Kloess J, Wharton S, Cattle N, Lackenby A, Daniels R, Hay A. 2010. Neuraminidase receptor binding variants of human influenza A(H3N2) viruses resulting from substitution of aspartic acid 151 in the catalytic site: a role in virus attachment? *J. Virol.* 84:6769–6781.
13. Zhu X, McBride R, Nycholat CM, Yu W, Paulson JC, Wilson IA. 2012. Influenza virus neuraminidases with reduced enzymatic activity that avidly bind sialic acid receptors. *J. Virol.* 86:13371–13383.
14. Gulati S, Smith DF, Cummings RD, Couch RB, Griesemer SB, St George K, Webster RG, Air GM. 2013. Human H3N2 influenza viruses isolated from 1968 to 2012 show varying preference for receptor substructures with no apparent consequences for disease or spread. *PLoS One* 8:e66325. doi:10.1371/journal.pone.0066325.
15. Hoffmann E, Neumann G, Kawaoka Y, Hobom G, Webster RG. 2000. A DNA transfection system for generation of influenza A virus from eight plasmids. *Proc. Natl. Acad. Sci. U. S. A.* 97:6108–6113.
16. Bloom JD, Gong LI, Baltimore D. 2010. Permissive secondary mutations enable the evolution of influenza oseltamivir resistance. *Science* 328:1272–1275.
17. Bao Y, Bolotov P, Dernovoy D, Kiryutin B, Zaslavsky L, Tatusova T, Ostell J, Lipman D. 2008. The influenza virus resource at the National Center for Biotechnology Information. *J. Virol.* 82:596–601.
18. Stamatakis A. 2006. RAXML-VI-HPC: maximum likelihood-based phylogenetic analyses with thousands of taxa and mixed models. *Bioinformatics* 22:2688–2690.
19. Drummond AJ, Suchard MA, Xie D, Rambaut A. 2012. Bayesian phylogenetics with BEAUti and the BEAST 1.7. *Mol. Biol. Evol.* 29:1969–1973.

20. Jones DT, Taylor WR, Thornton JM. 1992. The rapid generation of mutation data matrices from protein sequences. *Comput. Appl. Biosci. (Camb.)* **8**:275–282.
21. Martin J, Wharton SA, Lin YP, Takemoto DK, Skehel JJ, Wiley DC, Steinhauer DA. 1998. Studies of the binding properties of influenza hemagglutinin receptor-site mutants. *Virology* **241**:101–111.
22. Yang H, Chen LM, Carney PJ, Donis RO, Stevens J. 2010. Structures of receptor complexes of a North American H7N2 influenza hemagglutinin with a loop deletion in the receptor binding site. *PLoS Pathog.* **6**:e1001081. doi:[10.1371/journal.ppat.1001081](https://doi.org/10.1371/journal.ppat.1001081).
23. Das SR, Hensley SE, David A, Schmidt L, Gibbs JS, Puigbo P, Ince WL, Bennink JR, Yewdell JW. 2011. Fitness costs limit influenza A virus hemagglutinin glycosylation as an immune evasion strategy. *Proc. Natl. Acad. Sci. U. S. A.* **108**:E1417–1422.
24. Qiao H, Armstrong RT, Melikyan GB, Cohen FS, White JM. 1999. A specific point mutant at position 1 of the influenza hemagglutinin fusion peptide displays a hemifusion phenotype. *Mol. Biol. Cell* **10**:2759–2769.
25. Corti D, Voss J, Gamblin SJ, Codoni G, Macagno A, Jarrossay D, Vachieri SG, Pinna D, Minola A, Vanzetta F, Silacci C, Fernandez-Rodriguez BM, Agatic G, Bianchi S, Giacchetto-Sasselli I, Calder L, Sallusto F, Collins P, Haire LF, Temperton N, Langedijk JP, Skehel JJ, Lanzavecchia A. 2011. A neutralizing antibody selected from plasma cells that binds to group 1 and group 2 influenza A hemagglutinins. *Science* **333**:850–856.
26. Lai JC, Chan WW, Kien F, Nicholls JM, Peiris JS, Garcia JM. 2010. Formation of virus-like particles from human cell lines exclusively expressing influenza neuraminidase. *J. Gen. Virol.* **91**:2322–2330.
27. Rossman JS, Jing X, Leser GP, Lamb RA. 2010. Influenza virus M2 protein mediates ESCRT-independent membrane scission. *Cell* **142**:902–913.
28. Tappert MM, Porterfield JZ, Mehta-D'Souza P, Gulati S, Air GM. 2013. Quantitative comparison of human parainfluenza virus hemagglutinin-neuraminidase receptor binding and receptor cleavage. *J. Virol.* **87**:8962–8970.
29. Rogers GN, Herrler G, Paulson JC, Klenk HD. 1986. Influenza C virus uses 9-*O*-acetyl-*N*-acetylneuraminic acid as a high-affinity receptor determinant for attachment to cells. *J. Biol. Chem.* **261**:5947–5951.